J Fluoresc (2013) 23:1263–1269
DOI 10.1007/s10895-013-1259-x

ORIGINAL PAPER

A New Thiophenyl Pyrazoline Fluorescent Probe for Cu^{2+} in Aqueous Solution and Imaging in Live Cell

Meng-Meng Li · Wen-Bo Zhao · Ting-Ting Zhang · Wei-Liu Fan · Yu Xu · Yu Xiao · Jun-Ying Miao · Bao-Xiang Zhao

Received: 15 March 2013 / Accepted: 25 June 2013 / Published online: 7 July 2013

Abstract A new thiophenyl pyrazoline probe for Cu^{2+} in aqueous solution was synthesized and characterized by IR, NMR, HRMS and X-ray analysis. The probe displays remarkably high selectivity and sensitivity for Cu^{2+} with a detection limit of 1.919×10^{-7} M in aqueous solution (EtOH:HEPES = 1:1, v/v, 0.02 M, pH=7.2). In addition, the probe is further successfully used to image Cu^{2+} in living cells and the probe possesses good reversibility.

Keywords Pyrazoline · Fluorescent probe · Copper ion · Hela cell · Imaging

Introduction

Copper ion is one of essential heavy metal ions in human body and plays an important role in various physiologic processes [1, 2]. But disruption of copper homeostasis can result in a variety of diseases such as Menkes [3], Wilson's diseases [4], familial amyotropic lateral sclerosis [5], Alzheimer's disease [6], and prion diseases [7]. Moreover, long-term exposure to high levels of Cu^{2+} can induce liver and kidney damage [8]. Therefore, a sensitive method for detecting copper in biological samples is necessary and indispensable. A number of methods have been developed for the detection of copper, including atomic absorption spectrometry [9, 10], inductively coupled plasma atomic emission spectrometry [11, 12], voltammetry [13], electrochemical method [14, 15] and fluorescent chemosensors [16, 17]. However, most of these methods need relatively high cost apparatus and cannot be used in biological applications because they entail the destruction of the sample. Consequently, fluorescent chemosensors have attracted researchers' attention due to their high sensitivity, selectivity and easy operational use [18, 19].

Up to now, a lot of fluorescent sensors for monitoring Cu^{2+} based on calcein [20], rhodamine derivatives [21], Schiff base [22, 23], quinoline [24], fluorescein [25], coumarin [26, 27], indole [28] and naphthalendiimide [29] have been reported. However, major shortcomings of them are inferior selectivity [23], reversibility [22–25] or water solubility [26, 27]. Therefore, the development of water soluble and reversible fluorescent probes for monitoring Cu^{2+} in living cells is more appealing.

In recent years, pyrazoline derivatives have gained much attention due to their outstanding properties, such as high fluorescence quantum yields and excellent stability [30–34]. As an continuation of our work on the development of fluorescent probe for monitoring metal ions [33–37], herein we report a new pyrazoline-based fluorescent probe 3 (Scheme 1) for Cu^{2+} recognition. This probe with high sensitivity and selectivity for monitoring Cu^{2+} in aqueous solution is suitable for imaging Cu^{2+} in living cells.

Experimental Details

Apparatus

Thin-layer chromatography (TLC) was conducted on silica gel 60 F_{254} plates (Merck KGaA). ^{1}H NMR and ^{13}C NMR spectra were recorded on a Bruker Avance 300 (300 MHz

Meng-Meng Li and Wen-Bo Zhao contributed equally to this work.

Electronic supplementary material The online version of this article (doi:10.1007/s10895-013-1259-x) contains supplementary material, which is available to authorized users.

M.-M. Li · T.-T. Zhang · W.-L. Fan · Y. Xu · Y. Xiao · B.-X. Zhao (✉)
School of Chemistry and Chemical Engineering, Shandong University, Jinan 250100, People's Republic of China
e-mail: bxzhao@sdu.edu.cn

W.-B. Zhao · J.-Y. Miao (✉)
School of Life Science, Shandong University, Jinan 250100, People's Republic of China
e-mail: miaojy@sdu.edu.cn

Scheme 1 Synthesis of probe 3

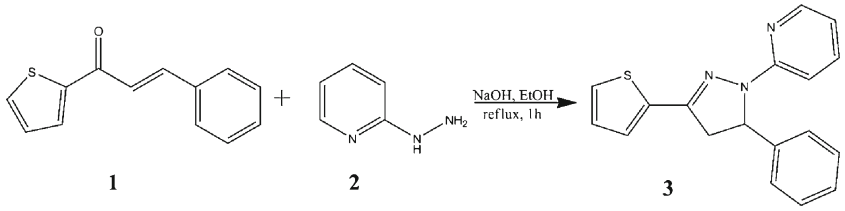

and 75 MHz) spectrometer, using DMSO as solvent, and tetramethylsilane (TMS) as internal standard. Melting points were determined on an XD-4 digital micro melting point apparatus. IR spectra were recorded with an IR spectrophotometer VERTEX 70 FT-IR (Bruker Optics). HRMS spectra were recorded on a QTOF6510 spectrograph (Agilent). UV–vis spectra were recorded on a U-4100 (Hitachi). Fluorescent measurements were recorded on a Perkin–Elmer LS-55 luminescence spectrophotometer. All pH measurements were made with a Model PHS-3C pH meter (Shanghai, China) and operated at room temperature about 298 K.

Reagents

Deionized water was used throughout the experiment. All the reagents were purchased from commercial suppliers and used without further purification. The salts used in stock aqueous solutions of metal ions were $NaNO_3$, $Fe(NO_3)_3\ 9H_2O$, $AgNO_3$, KNO_3, $Co(NO_3)_2\ 6H_2O$, $Mg(NO_3)_2\ 6H_2O$, $Ca(NO_3)_2\ 4H_2O$, $Al(NO_3)_3\ 9H_2O$, $Ba(NO_3)_2$, $Cr(NO_3)_3\ 9H_2O$, $Ni(NO_3)_2\ 6H_2O$, $Cd(NO_3)_2\ 4H_2O$, $Pb(NO_3)_2$, $Cu(NO_3)_2\ 3H_2O$, $Zn(NO_3)_2\ 6H_2O$ and $HgCl_2$.

Synthesis of 2-(5-Phenyl-3-Thiophen-2-yl-4,5-Dihydro-Pyrazol-1-yl)-Pyridine (3)

The synthetic route of proposed compound 3 is shown in Scheme 1. Starting materials chalcone (1) and 2-hydrazinylpyridine (2) were prepared according to literature [38, 39]. A mixture of chalcone (1) (0.419 g, 2 mmol), 2-hydrazinylpyridine (2) (0.258 g, 2.4 mmol), NaOH (0.250 g, 6 mmol) and ethanol (25 ml) was stirred at reflux for 1 h. After cooling, water (100 mL) was added to the mixture. The mixture was filtered and the crude product was crystallized from ethanol to give compound 3 as white crystals, Yield: 45.2 %; mp: 164–165 °C; IR (KBr, cm^{-1}): 3084.8, 2917.6, 1588.6, 1472.6, 1430.1, 1127.9, 766.0, 698.8; ^1H NMR (300 MHz, DMSO): δ 3.14 (dd, 1H, *J*=5.1, 17.4 Hz, 4-H*trans*), 3.91 (dd, 1H, *J*=12.3, 17.4 Hz, 4-H*cis*), 5.76 (dd, 1H, *J*=5.1, 12.3 Hz, 5-H of pyrazoline), 6.67 (t, 1H, *J*=6 Hz, pyridine-H), 7.11 (dd, 1H, *J*=3.6, 5.1 Hz, pyridine-H), 7.17–7.22 (m, 3H, Ar-H), 7.27 (s, 1H, Ar-H), 7.29–7.33 (m, 3H, Hz, thiophene-H), 7.96 (d, 1H, *J*=3.7 Hz, pyridine-H); ^{13}C NMR (75 MHz, DMSO): 155.33, 147.97, 146.63, 143.70, 137.86, 135.76, 129.03, 128.81, 127.34, 126.03, 114.86, 108.85, 60.87, 43.40. HRMS: calcd for $[M+H]^+$ $C_{18}H_{16}N_3S$: 306.1065; found: 306.1076.

A single crystal of 3 was obtained from ethanol solution and was characterized using X-ray crystallography (Fig.1).

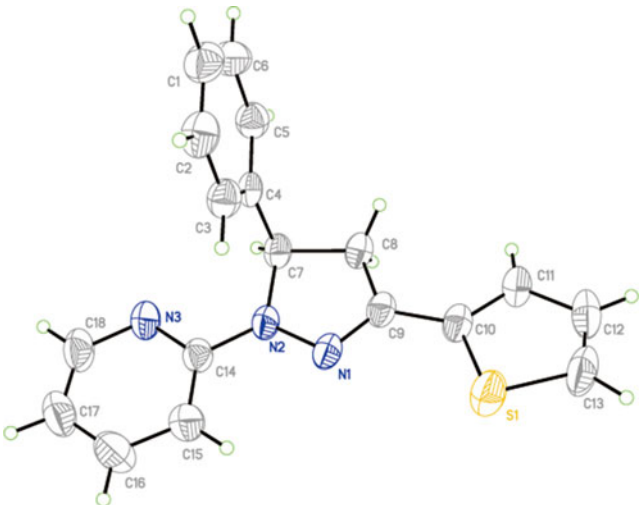

Fig. 1 Crystal structure of probe 3

Cell Culture and Imaging

Hela cells were cultured in Dulbecco's modified Eagle's medium (DMEM, Gibco) containing 10 % calf bovine serum

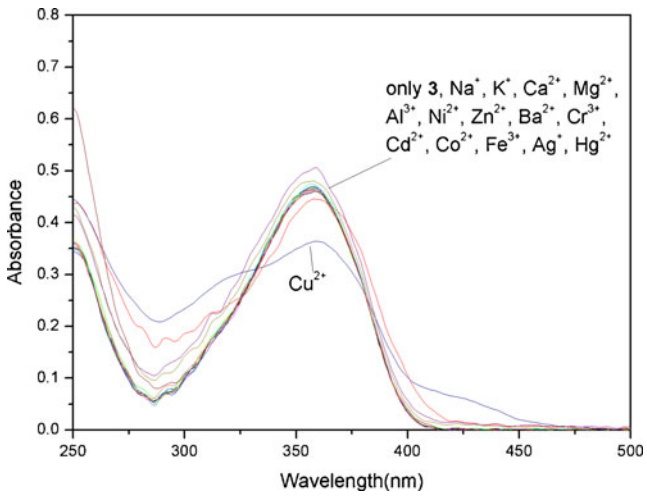

Fig. 2 Absorption spectra of probe 3 (10 μM) with addition of Al^{3+}, Fe^{3+}, Co^{2+}, Ni^{2+}, Ba^{2+}, Ca^{2+}, Cd^{2+}, Cr^{3+}, K^+, Mg^{2+}, Na^+, Ag^+, Hg^{2+}, Zn^{2+} and Cu^{2+} in aqueous solution (EtOH:HEPES=1:1, v/v, 0.02 M, pH=7.2) with an excitation at 356 nm

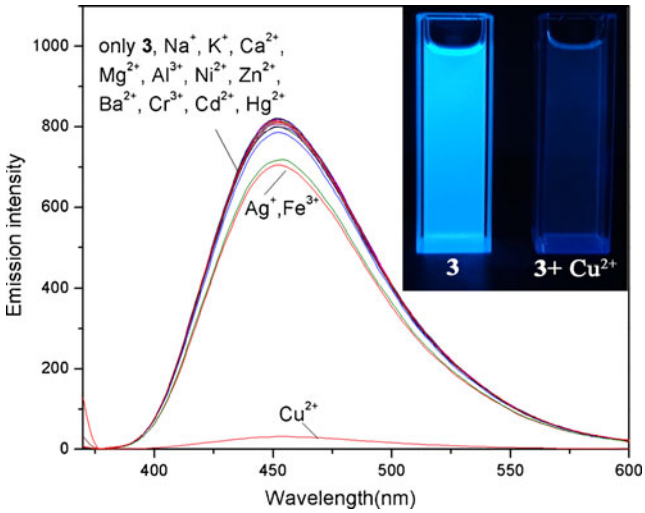

Fig. 3 Fluorescence spectra of probe 3 (10 μM) with addition of Al^{3+}, Fe^{3+}, Co^{2+}, Ni^{2+}, Ba^{2+}, Ca^{2+}, Cd^{2+}, Cr^{3+}, K^{+}, Mg^{2+}, Na^{+}, Ag^{+}, Hg^{2+}, Zn^{2+}, Cu^{2+} in aqueous solution (EtOH:HEPES 1:1, v/v, 0.02 M, pH=7.2) with an excitation at 356 nm and emission at 452 nm. Inset: the color change of probe 3 (10 μM) in aqueous solution (EtOH:HEPES 1:1, v/v, 0.02 M, pH=7.2) solution with 5 equiv. Cu^{2+}

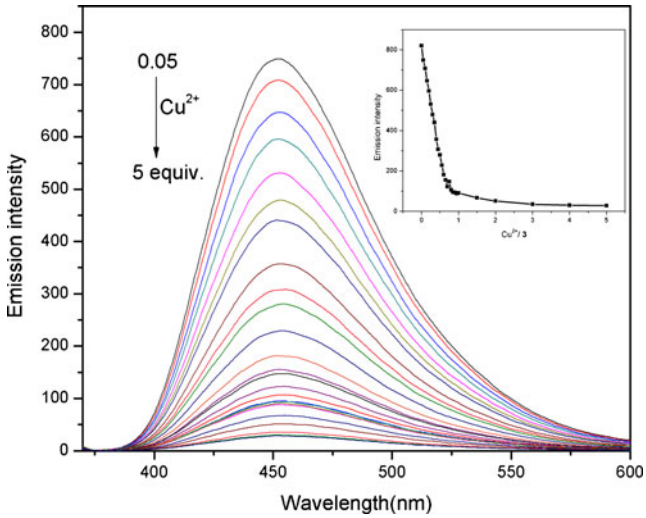

Fig. 5 Fluorescence spectra of probe 3 (10 μM) with addition of various concentrations of Cu^{2+} in aqueous solution (EtOH:HEPES=1:1, v/v, 0.02 M, pH=7.2) with an excitation at 356 nm

(HyClone) at 37 °C in humidified air and 5 % CO_2. For fluorescence imaging, the cells (5×10^4 mL^{-1}) were seeded into 24-well plates, and experiments to assay Cu^{2+} uptake were performed in the same media supplemented with 1 μM of $CuCl_2$ for 0.5 h. The cells were washed twice with PBS buffer before the staining experiments, and incubated with 1 μM of probe 3 for 1 h in the incubator. After washing twice with PBS, the cells were imaged under a Phase Contrast Microscope (Nikon, Japan).

Results and Discussion

Absorption Properties

The absorption spectra of probe 3 in aqueous solution (EtOH:HEPES=1:1, v/v, 0.02 M, pH=7.2) were investigated. As shown in Fig. 2, in the absence of Cu^{2+} ion, probe 3 showed an absorption maximum at 356 nm with ε 2.1×10^4 M^{-1} cm^{-1} (Fig. S1, Fig. S2). Upon the addition of Cu^{2+}, the absorption peak at 356 nm decreased with a red shift of 10 nm. Because of the binding of the probe and Cu^{2+}, conjugate electrons of the complex delocalized more than free

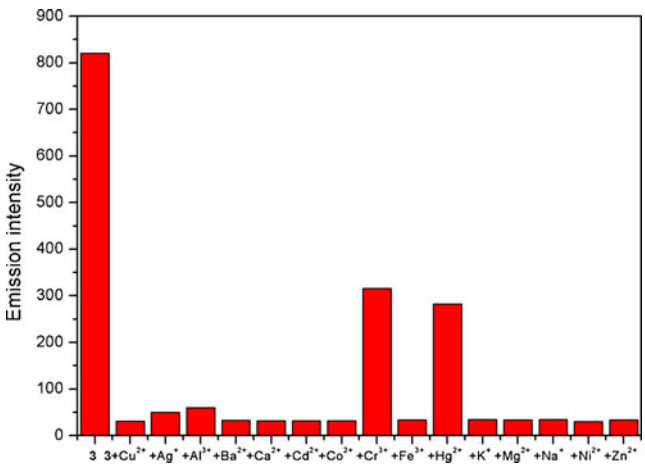

Fig. 4 Fluorescence spectra of probe 3 (10 μM) with addition of Al^{3+}, Fe^{3+}, Co^{2+}, Ni^{2+}, Ag^{+}, Hg^{2+}, Zn^{2+}, Ba^{2+}, Cd^{2+}, Cr^{3+} (5 equiv.) and Mg^{2+}, Ca^{2+} (100 equiv.) and K^{+}, Na^{+} (200 equiv.) in aqueous solution (EtOH:HEPES=1:1, v/v, 0.02 M, pH=7.2) containing 5 equiv. of Cu^{2+} with an excitation at 356 nm and emission at 452 nm

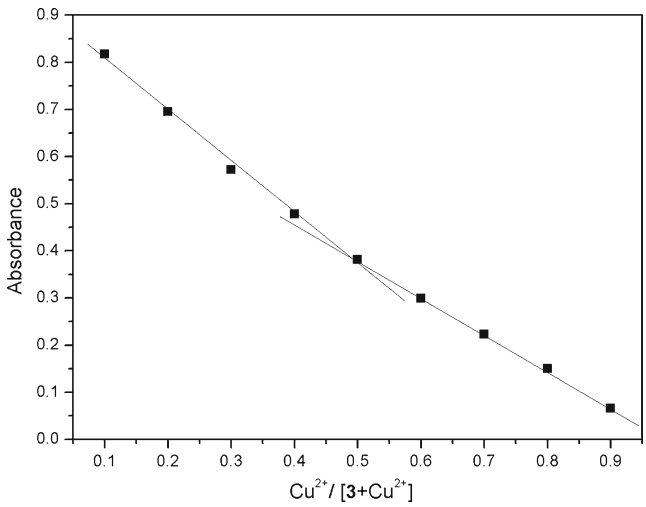

Fig. 6 Job's plot evaluated from the absorption spectra of probe 3 and Cu^{2+} in aqueous solution (EtOH:HEPES=1:1, v/v, 0.02 M, pH=7.2) with absorption at 356 nm (the total concentration of probe 3 and Cu^{2+} is 4.0×10^{-5} M)

Scheme 2 The proposed binding mode

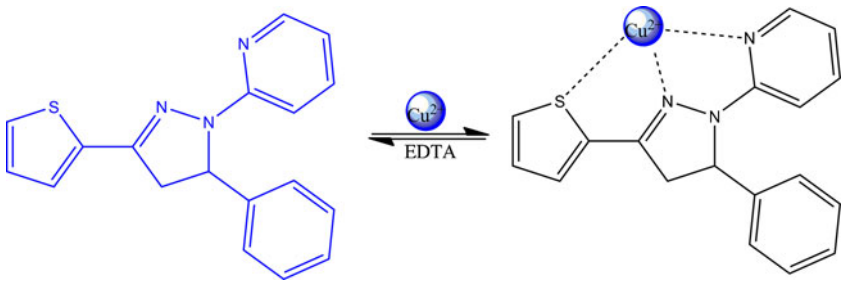

probe, resulting in a red shift of maximum absorption. It is obvious that none of other cations produced such a decrease in their absorption spectra.

Selectivity Studies

The fluorescence spectra of probe 3 with various metal ions in aqueous solution (EtOH:HEPES=1:1, v/v, 0.02 M, pH=7.2) were conducted to examine the selectivity. As shown in Fig. 3, the fluorescence spectra of probe 3 showed a strong fluorescence emission at 452 nm and the addition of 5 equiv. of Cu^{2+} induced a significant decrease in fluorescence intensity. However, the addition of other metal ions, including Al^{3+}, Fe^{3+}, Co^{2+}, Ni^{2+}, Ba^{2+}, Ca^{2+}, Cd^{2+}, Cr^{3+}, K^{+}, Mg^{2+}, Na^{+}, Ag^{+}, Hg^{2+}, Zn^{2+} did not induce obvious fluorescence change of the probe, which indicates the selectivity of the probe to Cu^{2+}. The fact was also confirmed by color change from stronger blue fluorescence in absence of Cu^{2+} to almost no-fluorescence in presence of Cu^{2+} under the irradiation at 365 nm. For other metal ions, no changes were observed under the same condition. Therefore, it also proved the selectivity of the probe to Cu^{2+} (Fig. 3 inset).

Anion effect on the selectivity of the probe for Cu^{2+} was also carried out. The results showed that the fluorescence intensity of 3-Cu^{2+} did not change in the cases of $CuSO_4$, $CuCl_2$, $Cu(NO_3)_2$ and $Cu(OAc)_2$ (Fig. S3).

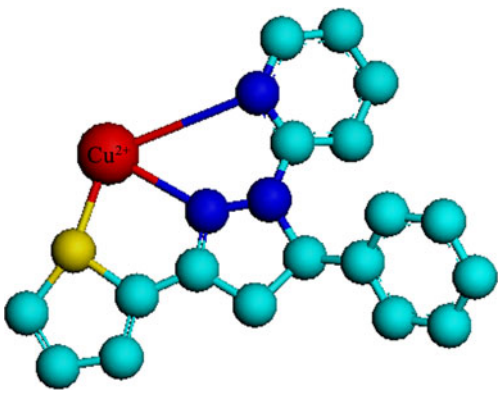

Fig. 7 Optimized structure of 3-Cu^{2+} by calculation

Tolerance Over Other Metal Ions

In order to test the practical application of the probe for Cu^{2+} ion, the interference of other common foreign ions on the fluorescence intensity of probe 3 was also studied. As shown in Fig. 4, only Cr^{3+} and Hg^{2+} slightly disturbed the fluorescence intensity of 3-Cu^{2+} and the initial fluorescence intensity of 3-Cu^{2+} did not change significantly with other metal ions such as Al^{3+}, Fe^{3+}, Co^{2+}, Ni^{2+}, Ba^{2+}, Ca^{2+}, Cd^{2+}, K^{+}, Mg^{2+}, Na^{+}, Ag^{+} and Zn^{2+}. The results indicated that probe 3 had a high selectivity for Cu^{2+} in the presence of other related species.

Cu^{2+}-Titration

As shown in Fig. 5, fluorescence titration experiments clearly showed fluorescence "turn-off". At the beginning, with the addition of Cu^{2+} at a concentration lower than 1.0 equiv. of probe 3, a significant decrease in the fluorescence intensity was observed and the fluorescence of probe 3 was almost completely quenched with only 2 equiv. of Cu^{2+} ions. As a

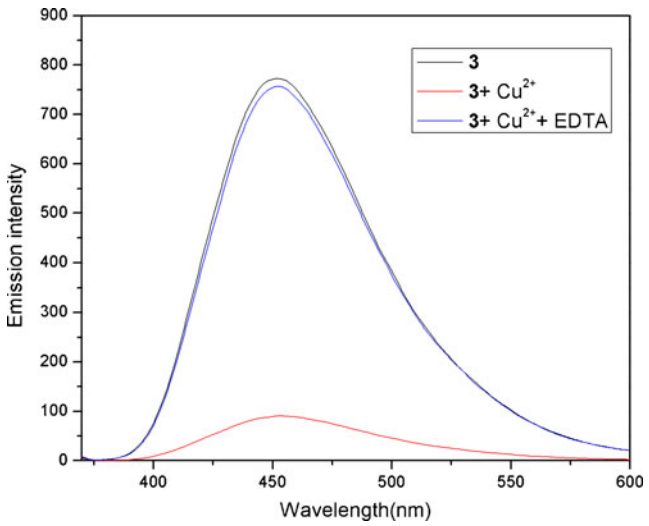

Fig. 8 Effect of EDTA (1 equiv.) on the fluorescence spectra of probe 3 (10 μM) with Cu^{2+} (1 equiv.) in aqueous solution (EtOH:HEPES=1:1, v/v, 0.02 M, pH=7.2) with an excitation at 356 nm and emission at 452 nm

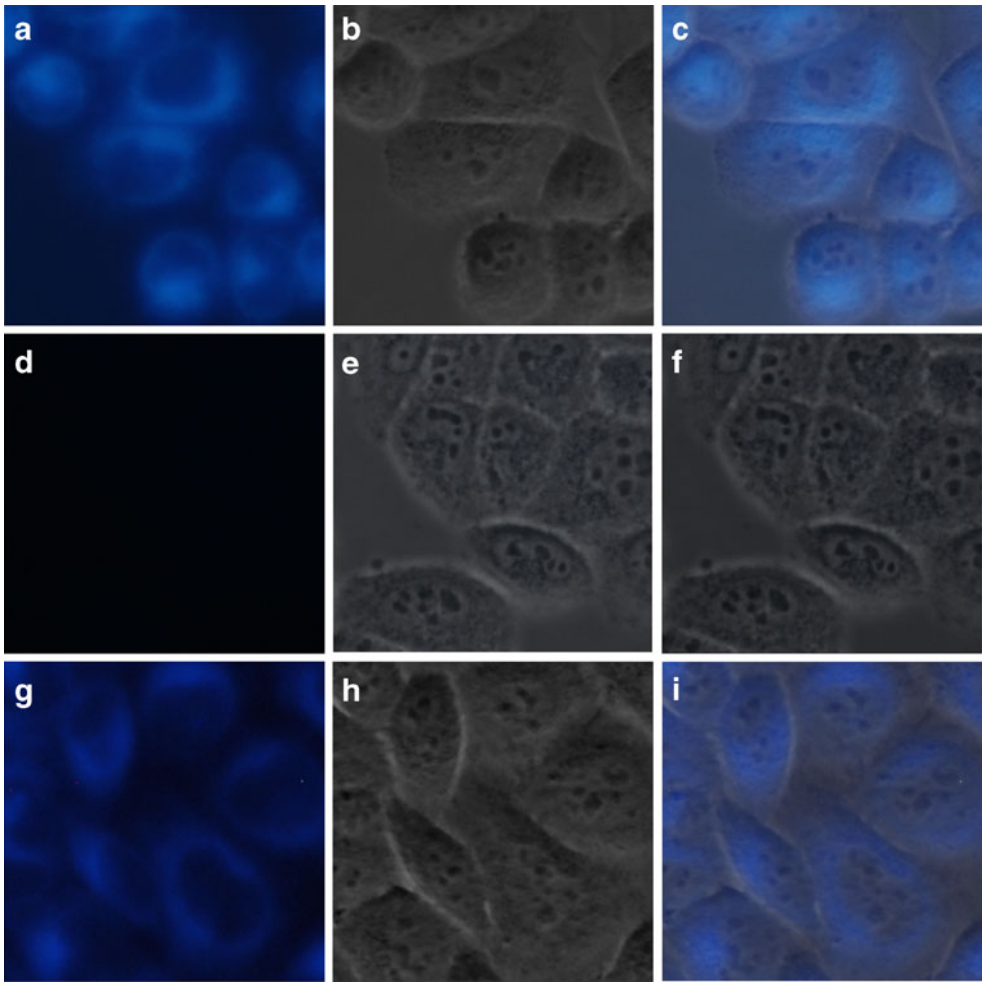

Fig. 9 Fluorescence microscope images of living Hela cells. a: Fluorescence image of probe 3 (1 μM); d: Fluorescence image of probe 3 (1 μM) in the presence of Cu^{2+} (1 μM); g: Fluorescence image of probe 3 (1 μM) in the presence of Cu^{2+} (1 μM) and EDTA (0.5 mM); b, e and h: Bright-field; c, f and i: Overlay image

further increase in Cu^{2+} concentration, the fluorescence intensity did not change (Fig. 5, inset). As shown in Fig. S5, the detection limit of probe 3 for the determination of Cu^{2+} was estimated to be 1.919×10^{-7} M (R=0.995). Therefore, the data demonstrate that compound 3 can be used as an excellent "turn-off" probe for detection of Cu^{2+} ion.

Binding of Probe 3 with Cu^{2+}

To investigate the coordination information between probe 3 and Cu^{2+}, the stoichiometry between probe 3 and Cu^{2+} in the complex system was determined by the changes in the absorption response of probe 3 with varying concentrations of Cu^{2+}. In Fig. 6, there is an inflection point when the molar fraction was 0.5, indicating a 1:1 stoichiometry of the Cu^{2+} to probe 3 in the complex. The association constant (Ka) of Cu^{2+} with probe 3 in HEPES buffered solution at pH 7.20 was found to be 6.796×10^{4} M^{-1} (Fig. S4). In addition, the Cu^{2+}-titration was also supposed a 1:1 Cu^{2+} complex formation. A proposed complex binding was presented in Scheme 2. Cu^{2+} was bound to one nitrogen atom from pyridine, one nitrogen atom from pyrazoline and one sulfur atom from thiophene. The model was confirmed by a theory calculation. Based on first-principles Density Functional Theory (DFT), the calculations were performed using the CASTEP code [40]. The exchange and correlation interactions were modeled using the generalized gradient approximation (GGA) with the PW91 functional [41]. In the geometrical optimization, all forces on atoms were converged to 0.05 eV Å, the maximum ionic displacement was within 0.002 Å and the total stress tensor was reduced to the order of 0.1 GPa (Fig. 7).

Reversibility and Effect of pH

The response of probe 3 to Cu^{2+} was confirmed to be reversible by the EDTA. As shown in Fig. 8, upon addition of 1 equiv. EDTA to the mixture of probe 3 (10 μM) and Cu^{2+} (10 μM) in aqueous solution (EtOH:HEPES=1:1, v/v, 0.02 M, pH=7.2), the fluorescent intensity was almost completely recovered, indicating that the EDTA replaced the receptor 3 to chelate Cu^{2+}. Thus, the experimental observations suggested that probe 3 should be a reversible for Cu^{2+}. On the other hand, the effect of pH on the fluorescence

response of probe 3 to Cu^{2+} was investigated. As shown in Fig. S5, in absence of Cu^{2+}, nearly no substantial change in fluorescence intensity of probe 3 was observed in the pH range from 5.5 to 9.0, but the fluorescence intensity of 3-Cu^{2+} has different responsive behaviors in different pH ranges. With increasing pH value from 5.5 to 7, the fluorescence intensity of 3-Cu^{2+} decreases because the deprotonation of probe 3 increases the conjugation between probe 3 and Cu^{2+}. The significant increase of the fluorescence intensity with the increasing pH value from 7.5 to 9.0 should be attributed to the displacing of Cu^{2+} from the complex, leading to the recovery of the fluorescence of probe 3. Thus, the coordination between probe 3 and Cu^{2+} is stable in the pH range of 7.0–7.5, indicating that the probe is promising for biological applications.

Imaging of Intracellular Cu^{2+}

The ability of probes to sensitively and selectively detect analyte in living cells is significant for biological application. Considering that higher level of Cu^{2+} in tumors takes a possible key role in promoting angiogenesis, we carried out assay in Hela cells.

From Fig. 9, we can clearly observe significant confocal imaging changes of probe 3 (1 μM) in the medium upon addition of Cu^{2+} (1 equiv.) for 1 h at 37 °C. Hela cells incubated with probe 3 initially display a strong fluorescent image, but the fluorescence image completely quenched in the presence of Cu^{2+}. When EDTA (0.5 mM) was added to the medium containing probe 3 (1 μM) and Cu^{2+} (1 μM), fluorescent image was returned because EDTA chelated strongly Cu^{2+} to lead to free probe 3.

Conclusions

In summary, a new pyrazoline-based probe 3 was developed. The probe can monitor Cu^{2+} with high sensitivity and selectivity over other competitive metal ions in aqueous solution (EtOH:HEPES=1:1, v/v, 0.02 M, pH=7.2). The binding ratio of probe 3 and Cu^{2+} was determined to be 1:1, which was confirmed by the Job's plot and the Cu^{2+}-titration results. The binding constant (*Ka*) for 3-Cu (II) was calculated to be $6.796\times 10^{4}\ M^{-1}$ and the detection limit of probe 3 for Cu^{2+} was 1.919×10^{-7} M. Additionally, the probe could serve as a reversible fluorescent probe to image Cu^{2+} in living cells.

Acknowledgments This study was supported by 973 Program (2010CB933504) and National Natural Science Foundation of China (90813022 and 20972088).

References

1. Robinson NJ, Winge DR (2010) Copper metallochaperones. Annu Rev Biochem 79:537–562
2. Que EL, Domaille DW, Chang CJ (2008) Metals in neurobiology: probing their chemistry and biology with molecular imaging. Chem Rev 108:1517–1549
3. Waggoner DJ, Bartnikas TB, Gitlin JD (1999) The role of copper in neurodegenerative disease. Neurobiol Dis 6:221–230
4. Camakaris J, Voskoboinik I, Mercer JF (1999) Breakthroughs and views molecular mechanisms of copper homeostasis. Biochem Biophys Res Commun 261:225–232
5. Bruijn LI, Miller TM, Cleveland DW (2004) Unraveling the mechanisms involved in motor neuron degeneration in ALS. Annu Rev Neurosci 27:723–749
6. Hung YH, Bush AI, Cherny RA (2010) Copper in the brain and Alzheimer's disease. J Biol Inorg Chem 15:61–76
7. Brown DR, Kozlowski H (2004) Biological inorganic and bioinorganic chemistry of neurodegeneration based on prion and Alzheimer diseases. Dalton Trans 33:1907–1917
8. Finkel T, Serrano M, Blasco MA (2007) The common biology of cancer and ageing. Nature 448:767–774
9. Gonzales APS, Firmino MA, Nomura CS, Rocha FRP, Oliveira PV, Gaubeur I (2009) Peat as a natural solid-phase for copper preconcentration and determination in a multicommuted flow system coupled to flame atomic absorption spectrometry. Anal Chim Acta 636:198–204
10. Budziak D, Silva EL, Campos SD, Carasek E (2003) Application of Nb_2O_5–SiO_2 in pre-concentration and determination of copper and cadmium by flow system with flame atomic absorption spectrometry. Microchim Acta 141:169–174
11. Liu Y, Liang P, Guo L (2005) Nanometer titanium dioxide immobilized on silica gel as sorbent for preconcentration of metal ions prior to their determination by inductively coupled plasma atomic emission spectrometry. Talanta 68:25–30
12. Guo Y, Din BJ, Liu YW, Changc XJ, Meng SM, Liu JH (2004) Preconcentration and determination of trace elements with 2-aminoacetylthiophenol functionalized Amberlite XAD-2 by inductively coupled plasma–atomic emission spectrometry. Talanta 62:207–213
13. Ensafi AA, Khayamian T, Benvidi A (2006) Simultaneous determination of copper, lead and cadmium by cathodic adsorptive stripping voltammetry using artificial neural network. Anal Chim Acta 561:225–232
14. Cheng WL, Sue JW, Chen WC, Chang JL, Zen JM (2010) Activated nickel platform for electrochemical sensing of phosphate. Anal Chem 82:1157–1161
15. Li C, Wang L, Deng L, Yu H, Huo J, Ma L, Wang J (2009) Electrochemical assessment of the interaction of dihydrogen phosphate with a novel ferrocenyl receptor. J Phys Chem B 113:15141–15144
16. Lai SJ, Chang XJ, Fu C (2009) Cadmium sulfide quantum dots modified by chitosan as fluorescence probe for copper (II) ion determination. Microchim Acta 165:39–44
17. Luo Y, Li Y, Lv BQ, Zhou ZD, Xiao D, Choi MMF (2009) A new luminol derivative as a fluorescent probe for trace analysis of copper (II). Microchim Acta 164:411–417
18. Pan M, Lin XM, Li GB, Su CY (2011) Progress in the study of metal–organic materials applying naphthalene diimide (NDI) ligands. Coord Chem Rev 255:1921–1936
19. Guerchais V, Fillaut JL (2011) Sensory luminescent iridium (III) and platinum (II) complexes for cation recognition. Coord Chem Rev 255:2448–2457
20. Liu M, Zhao HM, Quan X, Chen S, Yu HT (2010) Distance-independent quenching of quantum dots by nanoscale-graphene in self-assembled sandwich immunoassay. Chem Commun 46:1144–1146

21. Kumar M, Kumar N, Bhalla V, Sharma PR, Kaur T (2012) Highly selective fluorescence turn-on chemodosimeter based on rhodamine for nanomolar detection of copper ions. Org Lett 14:406–409
22. Aksuner N, Henden E, Yilmaz I, Cukurovali A (2009) A highly sensitive and selective fluorescent sensor for the determination of copper (II) based on a schiff base. Dye Pigment 83:211–217
23. Wen ZC, Yang R, He H, Jiang YB (2006) A highly selective charge transfer fluoroionophore for Cu^{2+}. Chem Commun 42:106–108
24. Liu ZP, Zhang CL, Wang XQ, He WW, Guo ZJ (2012) Design and synthesis of a ratiometric fluorescent chemosensor for Cu(II) with a fluorophore hybridization approach. Org Lett 14:4378–4381
25. Chen XT, Tong AJ (2012) Modification of silica nanoparticles with fluorescein hydrozide for Cu(II) sensing. Dye Pigment 95:776–783
26. Olimpo GB, Natalia M, Leidi CF, Jose Carlos NF, Vioctor V, Frank HQ, Marco TN, Bruce KC (2012) Design and synthesis of a new coumarin-based "turn-on" fluorescent probe selective for Cu^{2+}. Tetrahedron Lett 53:5280–5283
27. Ahamed BN, Ghosh P (2011) Selective colorimetric and fluorometric sensing of Cu (II) by iminocoumarin derivative in aqueous buffer. Dalton Trans 40:6411–6419
28. Kaur P, Kaur S, Singh K, Sharma PR, Kaur T (2011) Indole-based chemosensor for Hg^{2+} and Cu^{2+} ions: Applications in molecular switches and live cell imaging. Dalton Trans 40:10818–10821
29. Li QQ, Peng M, Li NN, Qin JG, Li Z (2012) New colorimetric chemosensor bearing naphthalendiimide unit with large blue-shift absorption for naked eyes detection of Cu^{2+} ions. Sensor Actuat B 173:580–584
30. Sarkar A, Bhattacharya SC (2012) Selective fluorescence resonance energy transfer from serum albumins to a bio-active 3-pyrazolyl-2-pyrazoline derivative: A spectroscopic analysis. J Lumin 132:2612–2618
31. Wang ML, Zhang JX, Liu JZ, Xub CX, Ju HX (2002) Intramolecular energy and charge transfer in 5-(9-anthryl)-3-(4-nitrophenyl)-1-phenyl-2-pyrazoline. J Lumin 99:79–83
32. Li MM, Huang SY, Ye H, Ge F, Miao JY, Zhao BX (2013) A new pyrazoline-based fluorescent probe for Cu^{2+} in live cells. J Fluoresc 23:799–806
33. Zhang Z, Wang FW, Wang SQ, Ge F, Zhao BX, Miao JY (2012) A highly sensitive fluorescent probe based on simple pyrazoline for Zn^{2+} in living neuron cells. Org Biomol Chem 10:8640–8644
34. Gong ZL, Ge F, Zhao BX (2011) Novel pyrazoline-based selective fluorescent sensor for Zn^{2+} in aqueous media. Sensor Actuat B 159:48–153
35. Liu WY, Li HY, Lv HS, Zhao BX, Miao JY (2012) A rhodamine chromene-based turn-on fluorescence probe for selectively imaging Cu^{2+} in living cell. Spectrochim Acta A 95:658–663
36. Liu WY, Li HY, Zhao BX, Miao JY (2012) A new fluorescent and colorimetric probe for Cu^{2+} in live cells. Analyst 137:3466–3469
37. Liu WY, Li HY, Zhao BX, Miao JY (2011) Synthesis, crystal structure and living cell imaging of a Cu^{2+}-specific molecular probe. Org Biomol Chem 9:4802–4805
38. Gresser R, Hartmann H, Wrackmeyer M, Leo K, Riede M (2011) Synthesis of thiophene-substituted aza-BODIPYs and their optical and electrochemical properties. Tetrahedron 67:7148–7155
39. Alhaider AA, Abdelkader MA, Lien EJ (1985) Design, synthesis and pharmacological activities of 2-substituted 4-phenylquinolines as potential antidepressant drugs. J Med Chem 28:1394–1398
40. Segall MD, Lindan PJD, Probert MJ, Pickard CJ, Hasnip PJ, Clark SJ, Payne MC (2002) First-principles simulation: ideas, illustrations and the CASTEP code. J Phys: Condens Matte 14:2717–2744
41. Mattsson AE, Armiento R, Schultz PA, Mattsson TR (2006) Nonequivalence of the generalized gradient approximations PBE and PW91. Phys Rev B 73:195123–195130